



Orbital Debris

Quarterly News

Volume 23, Issues 1 & 2
May 2019

Inside...

Centaur V Upper Stage
Fragmentation Update ... 2

2019 Fragmentations
Commence with Japanese
RB Breakup 3

ES-MCAT's Primary Mirror
Gets New Coating 3

Analysis of Stable LaPlace
Plane for Observation of
GEO Debris 4

Debris by the Numbers 6

New Geometry for Debris
Observations using
Goldstone OD Radar 8

Workshop Reports 9

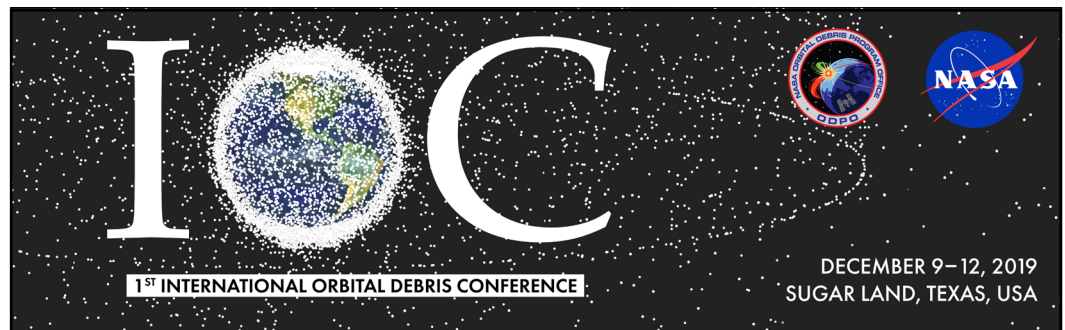
Abstract from the
NASA ODPO 10

Monthly Object Type
Charts by Number
and Mass 13

Space Missions/Satellite
Box Score 12, 14



A publication of
the NASA Orbital
Debris Program Office



The First International Orbital Debris Conference (IOC) is scheduled for December 9–12, 2019 at the Sugar Land Marriott Town Square in Sugar Land (greater Houston area), Texas.

The conference goal is to highlight orbital debris research activities in the United States and to foster collaborations with the international community. The 4-day conference will cover all aspects of micrometeoroid and orbital debris research, mission support, and other activities.

Visit the conference website for [registration](#) and [logistical](#) information.

<https://www.hou.usra.edu/meetings/orbitaldebris2019/>

2018 Ends with Breakup of an ORBCOMM Constellation Spacecraft

The seventh and last known breakup event of 2018 was noted on 22 December with the fragmentation of the ORBCOMM FM-16 spacecraft. This is the first known event for this bus/class of satellite. The event occurred with the parent spacecraft being in a 783 x 780 km, 45° orbit at the time.

The spacecraft (International Designator 1998-046E, U.S. Strategic Command [USSTRATCOM] Space Surveillance Network [SSN] catalog number 25417) is a first-generation ORBCOMM communications spacecraft, a member of the first so-called “little LEO” communication constellations. The spacecraft, shown in Fig. 1, used the Northrup Grumman (Orbital Sciences Corp.) MicroStar 40-kg

continued on page 2

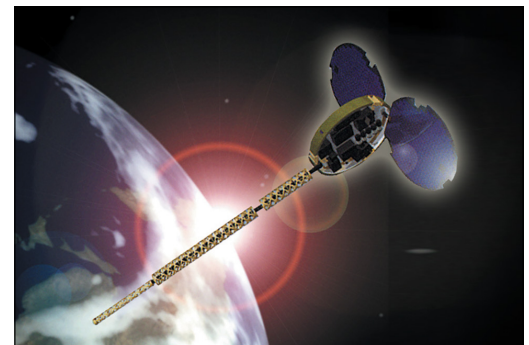


Figure 1. Artist's impression of a first-generation ORBCOMM spacecraft on-orbit. Visible are the main, circular body, the twin deployed solar array panels, and the nadir-pointing gateway antenna, subscriber antenna, and UHF beacon antenna/tip mass. Credit: ORBCOMM

ORBCOMM Constellation

continued from page 1

spacecraft bus. The spacecraft features an on-board Attitude Control System (ACS) that is responsible for attitude (antennas pointed to nadir) and solar array pointing. The ACS uses two torque rods and one coil to accomplish attitude control in concert with the gravity-gradient/antenna boom. In addition, a small gaseous nitrogen (GN2) thruster system and batteries compose the on-board stored energy complement, which could potentially contribute to an energetic fragmentation event.

In addition to the parent body, 12 debris (piece tags L-X inclusive) have entered the publicly-available U.S. Satellite Catalog. A Gabbard plot of this debris cloud is presented in Fig. 2. At the time of reporting, more than 30 pieces have been observed by the SSN sensor network. This piece count will be updated in the ODQN and in revisions to the NASA [History of On-orbit Satellite Fragmentations](#) as debris cloud cataloging develops. ♦

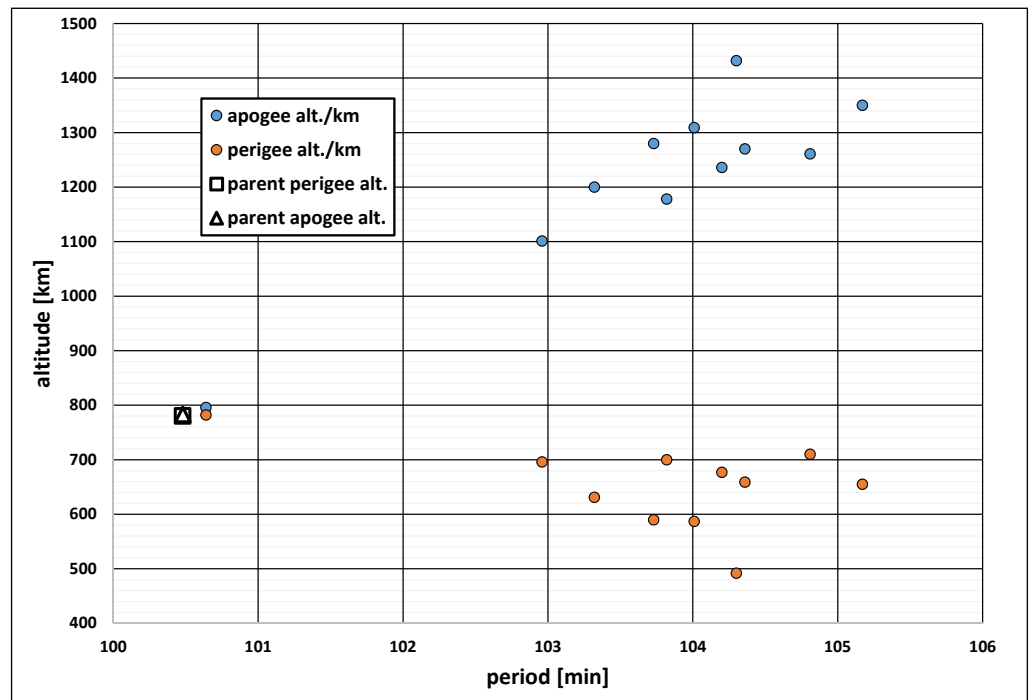


Figure 2. The ORBCOMM FM-16 Gabbard plot. Epoch is approximately 5 March 2019. Maximum change in period is on the order of 4.7 minutes. Maximum change in inclination is on the order of 0.5°, and all fragments entered higher-inclination orbits with respect to the parent body.

Centaur V Upper Stage Fragmentation Update

As reported in the last issue (ODQN, Vol. 22, Issue 4, p. 2), a Single-Engine Centaur

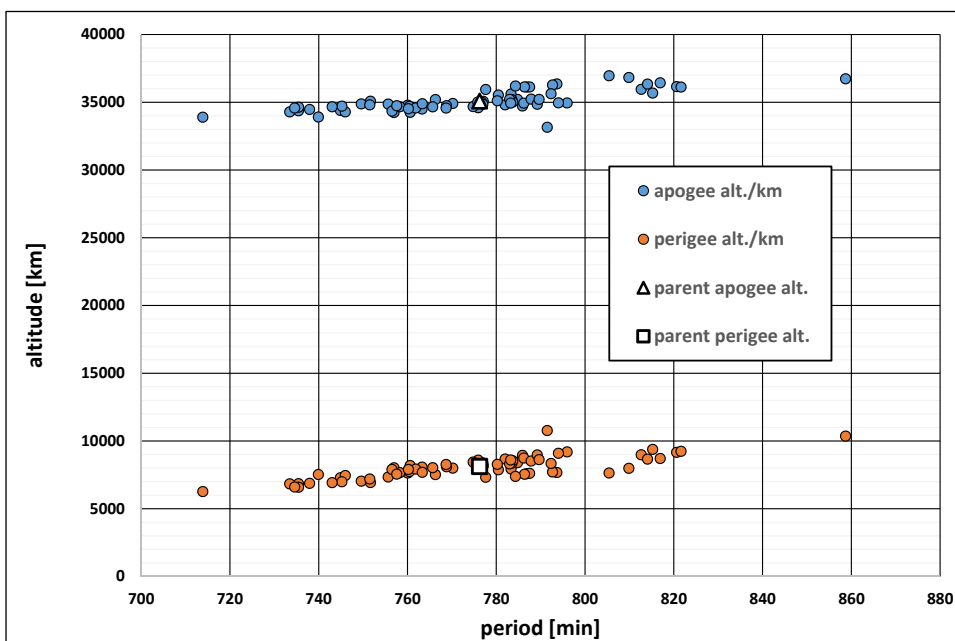
variant fragmented on 31 August 2018 after approximately 3.96 years on-orbit. This Centaur V

upper stage (International Designator 2014-055B, U.S. Strategic Command [USSTRATCOM] Space Surveillance Network [SSN] catalog number 40209) is associated with the launch of the USA 257 spacecraft from the U.S. Air Force Eastern Test Range. Two-line Element sets are now publicly available for the rocket body and 71 associated debris (piece tags C-CA). A Gabbard plot of this debris cloud is presented in the figure.

While technically this is the second breakup of a Centaur upper stage, the first event, Atlas Centaur 2 (1963-047A, SSN 694) in 1963, is not relevant due to its specifics (see reference) and the evolved nature of the modern Centaur vehicles. Three other Atlas V Centaurs have experienced aerodynamic breakups; only the aerodynamic breakup of the USA 230 rocket body on 17 August 2011 resulted in a single piece of short-lived, cataloged debris.

Reference

Anz-Meador, *et al.* "History of On-orbit Satellite Fragmentations (15th Edition)," NASA/TM-2018-2220037, (2018). ♦



The USA 257 R/B Gabbard plot. Epoch is approximately 5 March 2019. Maximum change in period is on the order of 82 minutes. Maximum change in inclination is on the order of 0.9° (one object), but average change was on the order of 0.03°.

2019 Fragmentations Commence with Japanese Rocket Body Breakup

Two distinct fragmentation events are associated with International Designator 2018-084, both apparently occurring on 6 February 2019. In this unusual circumstance, a Japanese H-2A second-stage rocket body experienced a breakup event, while a mission-related debris object experienced an anomalous object shedding event.

The rocket body, an H-2A model 202, (International Designator 2018-084L, U.S. Strategic Command [USSTRATCOM] Space Surveillance Network [SSN] catalog number 43682) launched the Japan Aerospace Exploration Agency GOSAT 2 primary payload and five small secondary payloads on 29 October 2018 and fragmented approximately 100 days after

launch. The rocket body was in a 590 x 493 km altitude, 98.8° orbit on the day of the event. The U.S. Consolidated Space Operations Center (CSpOC) reports a minimum of seven fragments associated with the breakup. The 3100 kg (dry mass) cryogenic stage's stored energy is normally minimized by standard stage passivation practices but the success of those practices in this case is unknown. One H-2 (1998-011B) and two H-2A second stages (2006-002B and -037B) have previously broken up.

The mission-related debris that experienced the anomalous event is piece tag E, SSN number 43675. The object is likely the conical "adapter" section of the three-section Kawasaki Heavy Industries 4/4D-LC dual Payload Encapsulation

System. The event occurred at 06:00 GMT on 6 February, while the object was in a 629 x 594 km altitude, 97.85° orbit. CSpOC observed five objects associated with this event. At least one prior higher-energy event, the breakup of mission-related debris object 2007-005E, is known and reported.

In addition to the parent bodies, four debris (piece tags M-Q inclusive) have entered the publicly-available U.S. Satellite Catalog; however, it is not clear at this time if these are associated with one or both of the parent bodies. This piece count will be updated in the ODQN and in revisions to the NASA [History of On-orbit Satellite Fragmentations](#) as debris cloud cataloging progresses. ♦

ES-MCAT's Primary Mirror Gets New Coating

The Eugene Stansbery Meter Class Autonomous Telescope (ES-MCAT) telescope is the proud recipient of a newly re-coated primary mirror. As with all visible telescopes with front-surface coated optics, periodic re-coating of the mirrors is required. Major research observatories typically strip/recoat mirrors every 1 to 5 years. With the harsh sea-level environment ES-MCAT is exposed to, it was determined that this maintenance was due in 2018. With the telescope nearing completion of testing planned for the Initial Operational Capability (IOC) phase, timing was ideal to recoat in preparation for attaining Full Operational Capability, anticipated for fall of 2019.

In May 2018, the NASA ES-MCAT optical team traveled to Ascension Island to remove the 800+lb, 1.3-m primary mirror from the telescope, and ship it to the ZeCoat Corporation in Torrance, California. ZeCoat coated the mirror with an enhanced, protected silver, multi-layer coating with an average reflectivity of >95% across the visible spectral bands employed by ES-MCAT (360 – 1000 nm). Not only is the performance significantly better than protected aluminum (ES-MCAT's original coating), but extensive environmental tests demonstrated this proprietary silver coating is also much more durable. Originally patented by Lawrence Livermore National Labs [1], the coating was re-developed by ZeCoat for NASA, employing an ion-assisted evaporation process for easy application to meter-class mirrors [2]. This



Figure 1. ES-MCAT's primary mirror in the lab at ZeCoat Corporation. The new, enhanced, protected silver coating is both more environmentally durable and more reflective throughout visible-bands (>95% average reflectivity).

coating was previously applied by ZeCoat to the 1.44-m Kepler Space Telescope as well as JPL's Moon Mineralogy Mapper spectrometer mirror.

In December 2018, the NASA ES-MCAT team returned with DFM Engineering, who designed, built, and installed ES-MCAT, for the week-long process to carefully

reinstall the mirror into the mirror cell and hoist it up to the telescope. The mirror was aligned, mechanically/laser collimated, and collimated on-sky. Initial tests indicate that ES-MCAT's performance with the new silver-coated mirror now exceeds its previous best performance with the original aluminum coating. Testing is ongoing to quantify how capable ES-MCAT has become.

References

1. Wolfe, J. D. and Thomas, N. L. "Durable silver coating for mirrors." U.S. Patent No. 6,078, p. 425, (20 Jun. 2000).
2. Sheikh, D. A., Connell, S. J., Dummer, R. S. "Durable silver coating for Kepler Space Telescope primary mirror." Proc. SPIE 7010, *Space Telescopes and Instrumentation 2008: Optical, Infrared, and Millimeter*, 70104E (July 12, 2008); doi:10.1117/12.789996. ♦

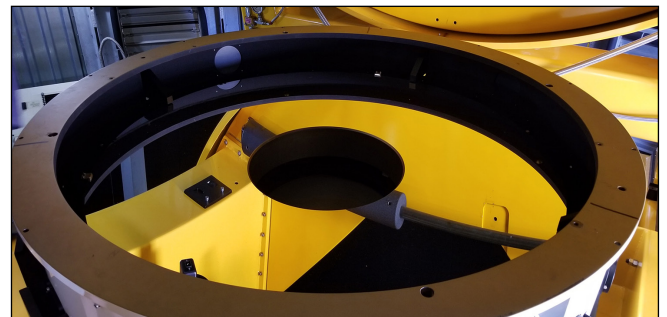


Figure 2. The 800+lb mirror installed in the mirror cell attached to the telescope.

PROJECT REVIEW

Analysis of the Stable Laplace Plane for the Observation of Geosynchronous Debris

D. GATES AND J. FRITH

It has long been known that objects in geosynchronous orbits (GEO) are subject to perturbations due to the oblateness (equatorial bulge) of the Earth, third-body gravitational interactions induced by the Sun and the Moon (lunisolar perturbations), and solar radiation pressure (SRP) [1,2,3,4]. These forces cause the orbit to precess in inclination and right ascension of ascending node (RAAN), *e.g.*, the oblateness of the Earth causes a precession of the orbit in a reference plane about Earth's pole of rotation. Indeed, the combined interaction of these forces on a near-GEO object causes the orbit to simultaneously precess around multiple axes. A natural question is then whether or not a stable reference plane can be found in which the orbit of these objects appears to be frozen, *i.e.*, the orbit maintains a constant tilt or inclination with respect to the reference plane. Such a plane is called the classical Laplace plane. It is the plane at a particular geocentric distance where the effects of oblateness and lunisolar forces are equal.

The classical Laplace plane solution does not include the effects of SRP, which dominate the short-term evolution of typical debris orbits [2, 3, 4]. Thus, a modification to the classical Laplace plane is required. The GEO propagator used by the NASA Orbital Debris Program Office (ODPO) to evolve the orbits of GEO objects and debris was used to simulate the evolution of objects through a set of possible Laplace inclinations (see Fig. 1). The propagator evolves the orbits and includes the effects of oblateness, lunisolar perturbations, and SRP. SRP is a function of the flux density of solar radiation at the distance of the Earth and depends upon the reflectivity and surface area of an object. The amount of radiation pressure caused by the reflectivity of the object, *i.e.*, the photon momentum transfer, varies from 0.0 (completely transparent) and 2.0 (perfect flat mirror). We used a reflection coefficient of 1.1, typical of an absorber.

For this study, we analyzed the stability of the Laplace plane by calculating the maximal Lyapunov coefficient (LCE) for a test orbit. The LCE characterizes the rate of exponential divergence from perturbed initial conditions by a system. Consider the cases of two orbits, $x(t)$ and $x_s(t)$. Let x_s be a small variation ϵ away from x and call this orbit a "shadow" orbit as it shadows

the orbit of interest. At some time τ , after evolving the system from an initial time t , the divergence between these two paths increases exponentially as:

$$\|x(t + \tau) - x_s(t + \tau)\| = \|x(t) - x_s(t)\|e^{\lambda\tau}$$

where λ is the LCE. Negative LCE systems subsequently are considered to be stable and positive valued LCE systems to be unstable.

continued on page 5

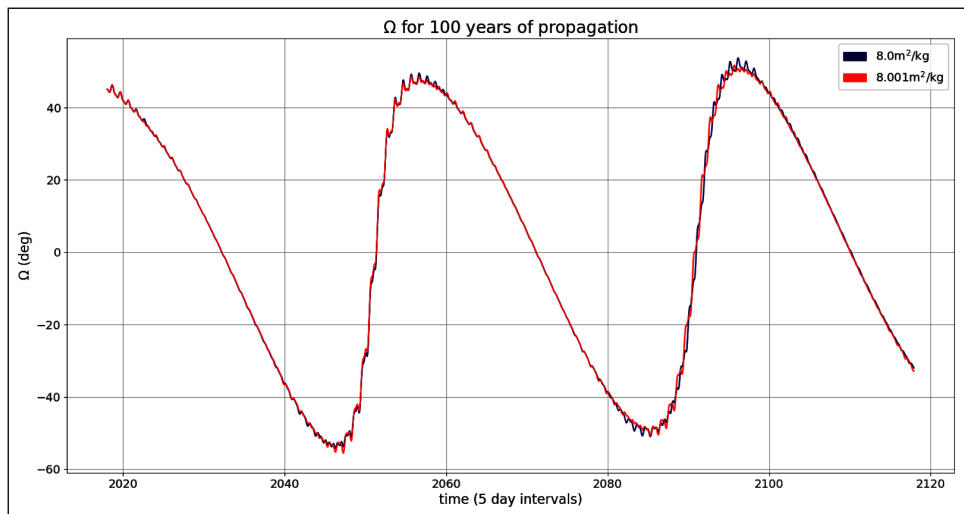


Figure 1. 100-year propagation of two GEO objects, $e = 0.0001$, $a = 42,000$ km, $A/m = 8.0$ m²/kg with lunisolar, oblateness, and SRP effects of right ascension of ascending node (RAAN) vs time. We chose $A/m = 8.0$ m²/kg as an example because the system is chaotic at this A/m ratio. The curves are in right ascension vs. time space and show divergences at the minimum and maximum after 80 years of propagation. Note that this is an exaggerated example, as typically the choice of perturbation for the "shadow" orbit is on the order of 10^{-9} from the initial state for all elements of an orbit of interest.

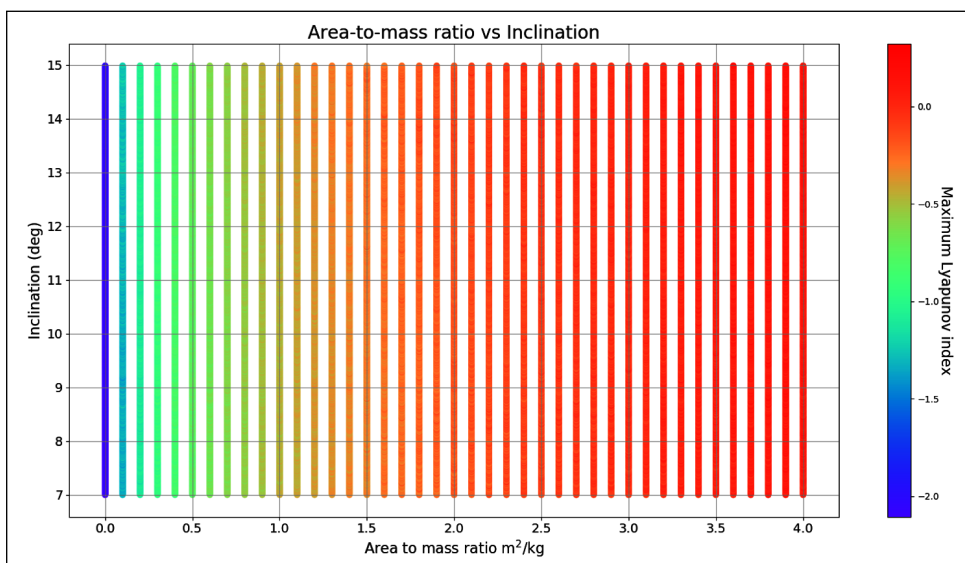


Figure 2. 100-year propagation of a GEO object, eccentricity equal to 0.0001 and a semi-major axis equal to 42,000 km. The chart shows A/m ratio vs. inclination in discrete vertical bars at each one of 40 A/m ratios between 0.0 m²/kg and 4.0 m²/kg and inclinations between 7.0° and 15.0°. The vertical bars have a color map applied across them corresponding to their associated Lyapunov coefficient. From this color map, it is clear that the Lyapunov coefficient increases with increasing A/m ratio as expected.

Analysis of Stable Laplace Plane

continued from page 4

We propagated sample debris orbits over 100 years with 5-day time steps, with chosen A/m ratios, at all inclinations between 7.0° and 15.0° in step sizes of 0.01° . To find the LCE for a given orbit of interest, one evolves the orbit in time with a “shadow” orbit, varying in initial conditions by some small amount, typically on the order of 10^{-9} , and then determines the logarithmic divergence of the two paths over time (Fig. 1). For sufficiently many time steps, N , the sum of these divergences is the LCE. For this study, we used the Rosenstein-Kantz algorithm [5] to calculate the maximal LCE, whereby one sums over the logarithm of the difference between the reference orbit and the “shadow” orbit and divides by the amount of initial variation between x_i and x_s , ϵ . The final coefficient is then the sum divided by the product of the number of steps taken N and time step size τ :

$$\lambda = \lim_{N \rightarrow \infty} \frac{1}{N * \tau} \sum_{j=1}^N \ln \frac{||x - x_s||}{\epsilon}$$

For an object with a semi-major axis of 42,000 km and an initial eccentricity of 0.0001, we found LCE's for A/m ratios of GEO objects from $0.0 \text{ m}^2/\text{kg}$ (as a reference) to $4.0 \text{ m}^2/\text{kg}$ and the corresponding Laplace loci (Fig. 2). A Laplace locus corresponds to the frequency of the time steps in which the object is near its initial RAAN, which means the observation of such an object is more likely for a fixed pointing geometry. Since the LCE measures the stability of an orbit, it is suitable for quantifying the stability of the Laplace plane.

As an example, consider the stability of the theoretical Laplace plane at 7.2° inclination (Fig. 3). The plane destabilizes for an A/m ratio of $3.1 \text{ m}^2/\text{kg}$, so it follows that observing orbital debris with A/m ratios above this value in the classical Laplace plane is not as likely because such objects spend less time in that plane. Since we are interested in maximizing the chance of observing orbital debris, predicting the Laplace plane for any given A/m ratio is paramount. Such planes were found for each A/m ratio considered by calculating the minimal (*i.e.*, most stable) Lyapunov coefficient and the associated inclination at which such a point occurred. Then, a curve was fit to the data using a 3rd order Hermite polynomial (Fig. 4).

Of interest to the ODPO [2, 3] is the observation of high area-to-mass (HAMR) debris, *e.g.*, multi-layer insulation. Therefore, we extrapolated the Laplace plane for HAMR

debris from Fig. 4. Subsequent analysis found that the extended curve agrees well with theoretical values from Rosengren, *et al.* [4] and is suitable for predicting the Laplace plane of HAMR debris with A/m ratios up to $35 \text{ m}^2/\text{kg}$ and semi-major axes between 40,000 km and 44,000 km.

One important result of this study is that as the A/m ratio increases, the location of the center of oscillations and the corresponding approximate Laplace plane shift positions to higher inclinations (Fig. 4). This should have a significant effect on the

planning for observations of HAMR GEO debris so that the HAMR population is more thoroughly sampled. Additionally, these results will help direct future modifications to the ODPO model assumptions with the goal of ultimately providing a more accurate estimation of the long-term risk GEO debris has on operational, GEO assets and the space environment in general.

continued on page 6

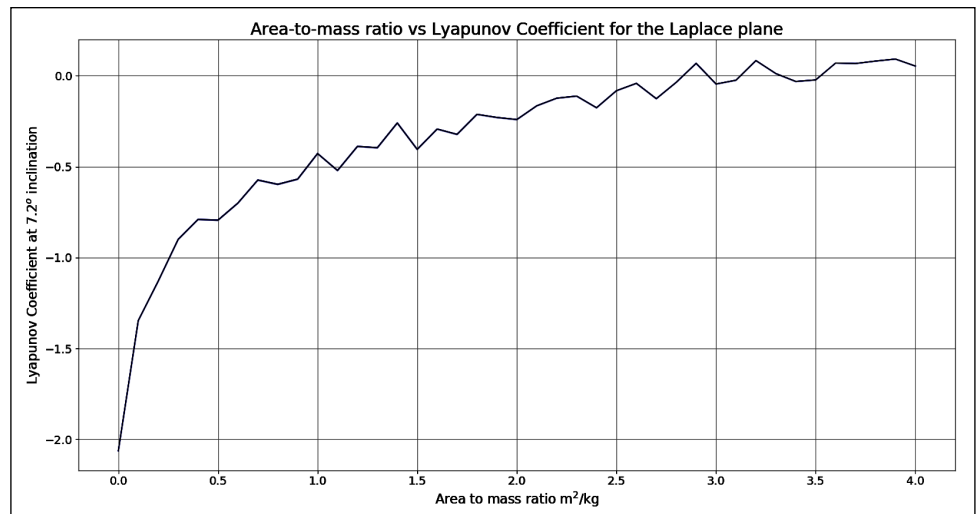


Figure 3. A/m ratio vs. Lyapunov coefficient for the classical Laplace Plane. This figure is the result of extracting the 7.2° inclination data from Fig. 2. This chart shows how the Laplace plane destabilizes as A/m ratio increases, eventually becoming unstable at $\sim 3.1 \text{ m}^2/\text{kg}$ as the LCE becomes positive. This marks the transition from the LAMR to the HAMR regime as the classical Laplace plane destabilizes above this A/m ratio for an object with a semi-major axis of 42,000 km.

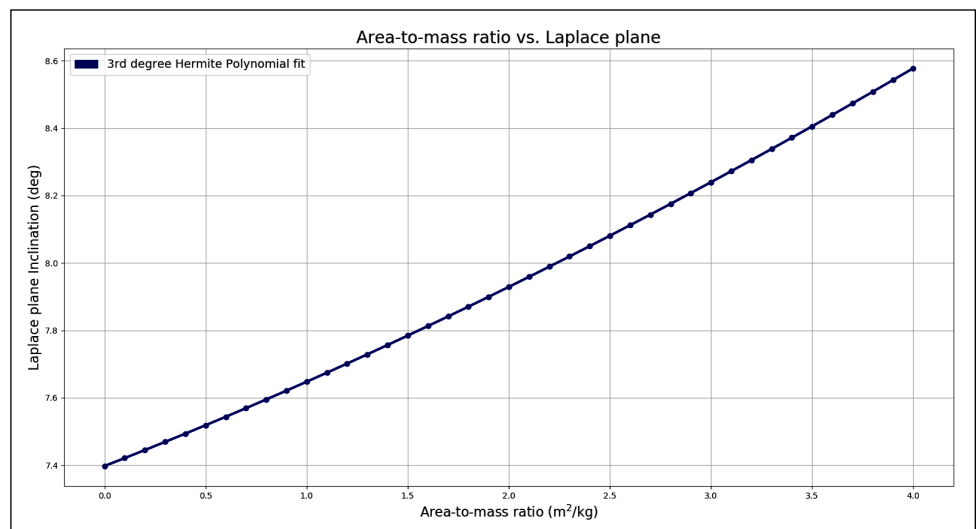


Figure 4. 3rd Degree Hermite polynomial curve fit of A/m ratio vs. the Laplace plane for $a=42,000 \text{ km}$, where the Laplace plane is defined as the inclination at which the Lyapunov coefficient is minimized for a reference A/m ratio. The coefficients of the Hermite series are: $p(x) = c_0 + c_1 H_1(x) + c_2 H_2(x) + c_3 H_3(x)$ are $c_0 = 7.30717121$, $c_1 = 1.33787928e-01$, $c_2 = 3.56525340e-03$, and $c_3 = -3.72481230e-05$.

Analysis of Stable Laplace Plane

continued from page 5

References

1. Allan, R.R. and Cook, G.E. "The long-period motion of the plane of a distant circular orbit," *Proc. R. Soc. Lond. A*, Vol. 280, pp. 97-109, (1964).
2. Friesen, J, Albert, L.J., and Kessler, D., *et al.* "Analysis of orbital perturbations acting on objects in orbits near geosynchronous

Earth orbit," *Journal of Geophysical Research*, 97, 10.1029/92JE00032, (1992).

3. Liou, J.-C. and Weaver, J.K. "Orbital Dynamics of High Area-to-Mass Ratio Debris and their Distribution in the Geosynchronous Region," *Proceedings of the 4th European Conference on Space Debris (ESA SP-587)*, ESA/ESOC, Darmstadt, Germany, p. 2851, (2005).

4. Rosengren, A.J., Scheeres, D.J., and McMahon, J.W. "The Classical Laplace Plane and its use as a Stable Disposal Orbit for GEO," *Adv. Space Res.*, Vol. 53, pp. 1219-1228, (2004).

5. Kantz, H. "A robust method to estimate the maximal Lyapunov exponent of a time series," *Physics Letters*, Vol. 185, Issue 1, pp. 77-87, (31 January 1994). ♦

Debris by the Numbers: a Précis of the NASA History of On-orbit Satellite Fragmentations, 15th Ed.

P. D. ANZ-MEADOR

Since the publication of the 14th edition of the NASA Orbital Debris Program Office's (ODPO) History of On-orbit Satellite Fragmentations (HOOSF), fragmentation events—some of a major magnitude—have continued the growth

of the orbital debris complex. The 14th edition (14/e), with an information cut-off date of 1 August 2007, [1] and the 15th edition (15/e), with an information cut-off date of 4 July 2018, [2] provide a comparative opportunity to examine and understand that growth. Figure 1 compares

the number of yearly events in the two editions, 193 (14/e) to 242 (15/e), as well as four further events since the 15th edition's publication.

Note that several years covered by the 14th edition display additional breakups. This is because new events were recognized as occurring in the historical years or were formally acknowledged to be breakup events. This is indicative of the value of monitoring the Department of Defense (DOD) Space Surveillance Network catalog and recognizes the close partnership between ODPO and the DOD surveillance and resident space object (RSO) tracking and cataloging authorities. Further historical events may be recognized in future editions.

The 10 largest events (based on in-orbit debris at the information cut-off dates) replace four of the 14th edition's events with more recent, larger-magnitude events principally, but not exclusively, due to the accidental collision of two communication spacecraft in 2009. While the effects of 38% of all breakups have completely disappeared, only 10 of the 5385 space missions flown since 1957 are responsible for 33% of all cataloged artificial Earth satellites presently in orbit. Moreover, the sources of four of these 10 fragmentations were discarded rocket bodies that had operated as designed, but later broke up.

Modern debris mitigation best practices likely would have prevented these events. The remaining six fragmentations are diverse in character. The oldest, the fragmentation of Cosmos 1275, is

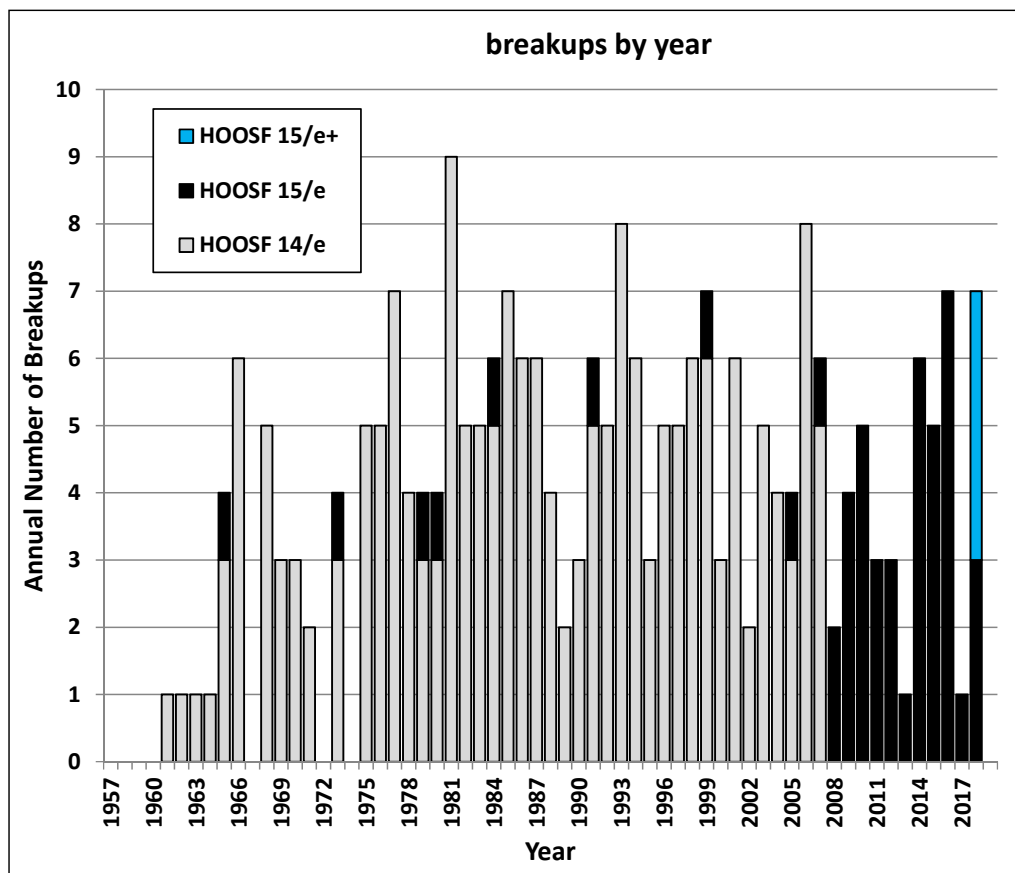


Figure 1. A comparison of known breakups in the 14th and 15th editions of the HOOSF. Note that the "HOOSF 15/e+" category consists of 2018 events occurring after the 4 July 2018 cut-off date.

continued on page 7

Debris by the Numbers

continued from page 6

assessed by Russian authorities to have been caused by a battery fragmentation. Two, USA 109 and NOAA 16, share a similar spacecraft bus. More recently, the intentional destruction of the Fengyun-1C (FY-1C) meteorological payload (1999-025) by an anti-satellite (ASAT) weapon and the first accidental collision of large intact spacecraft, Cosmos 2251 (1993-036) and Iridium 33 (1997-051), together account for over 30% of all cataloged RSOs. The breakup fragments associated with these three spacecraft account for almost 13% of all objects cataloged since the launch of Sputnik 1 on 4 October 1957.

Figure 2 illustrates the 4 July 2018 percentages associated with major RSO-type categories. The reader is reminded that absolute

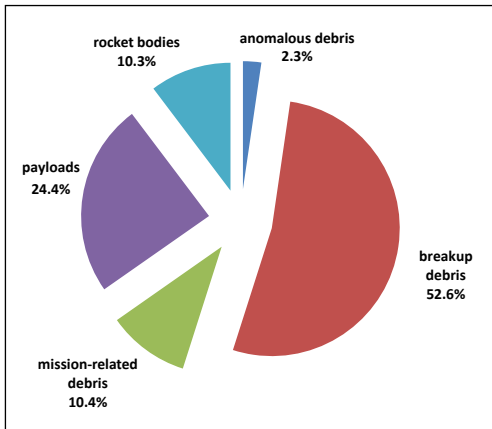


Figure 2. Relative segments of the cataloged in-orbit (4 July 2018) Earth satellite population. Anomalous debris is produced in unplanned events that result in the separation, usually at low velocities, of one or more objects from the parent body. Mission-related debris results from the intentional release of objects during nominal on-orbit operations.

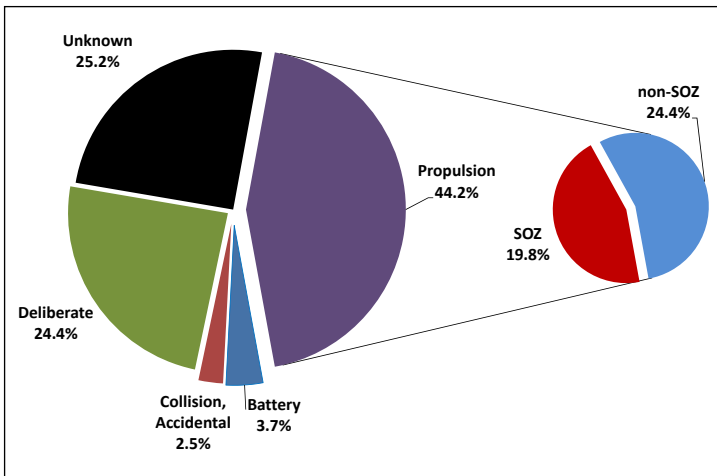


Figure 3. Causes of the 242 known satellite breakups.

numbers or percentages are subject to debris cataloging constraints, as well as the difficulty in tracking and cataloging debris in highly elliptical and deep space orbits.

The primary causes of satellite breakups, enumerated in Fig. 3, are propulsion-related events and deliberate actions, although the cause for almost one in four breakups remains unknown. Deliberate actions, often associated with activities related to national security, were formerly the most frequently occurring class, although only one such event occurred during the decade from 1997 until the FY-1C event. Propulsion-related breakups, currently the most frequent class, include catastrophic malfunctions during orbital injection or maneuvers, subsequent explosions based on residual propellants, and failures of active attitude control systems.

Breakups of rocket bodies due to propulsion failures are usually more prolific and produce longer-lived debris than the intentional destruction of payloads, often due to the higher altitudes of the malfunctioning rocket bodies rather than the mechanics of the explosive event. Breakups of the Russian Federation’s Blok-DM *Sistema Obespecheniya Zapuska* (SOZ) ullage motors, regularly reported in the Orbital Debris Quarterly News, are segregated from other members of the propulsion ensemble due to their high probability of fragmentation, which tends to overinflate the propulsion category to some degree; omitting the SOZ breakups equates the non-SOZ propulsion and deliberate categories.

Although it may appear obvious that a rocket body breakup should be classified under the “Propulsion” category, rocket body events are carried as “Unknown” until a failure mechanism can be confidently identified for that rocket body design and is associated with a given rocket body event.

On average, the resulting debris from

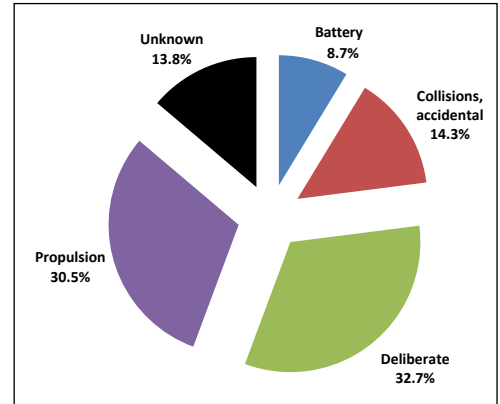


Figure 4. Proportion of cataloged satellite breakup debris remaining in orbit. The “deliberate” category predominates due to the FY-1C ASAT event.

historical deliberate actions is short-lived, the exception again being FY-1C. Figure 4 illustrates the 4 July 2018 proportions of in-orbit cataloged breakup debris.

Examining the sources of satellite breakup debris in-orbit by satellite type, payloads (63%) have now supplanted rocket bodies (34.6%) as the predominant source of breakup debris remaining in orbit. The balance is attributed to mission-related debris.

The percentage distribution is driven primarily by the intentional (FY-1C) and accidental (Iridium 33 and Cosmos 2251) collision’s payload breakup events. This does not diminish, in any way, the imperative for launch providers and spacecraft owner/operators to lessen the probability of accidental fragmentation by employing robust root-cause analysis to identify existing or potential failure modes, reviewing and updating design best practices on a regular basis, and incorporating design lessons learned into the life cycle of spacecraft and rocket bodies in a timely fashion. Pro-active design and operational procedures, when implemented, have proven their worth by demonstrably reducing fragmentations over multiple launch agencies and vehicle types.

References

1. Johnson, N., et al. “History of On-orbit Satellite Fragmentations (14th Edition),” NASA/TM-2008-214779, (2008).
2. Anz-Meador, P., et al. “History of On-orbit Satellite Fragmentations (15th Edition),” NASA/TM-2018-2220037, (2018). ♦

New Geometry for Debris Observations using the Goldstone Orbital Debris Radar

J. MURRAY

The Goldstone Orbital Debris Radar has been collecting orbital debris data for the NASA Orbital Debris Program Office since 1990. It is operated in a staring mode designed to statistically sample objects in low Earth orbit (LEO, the region below 2000 km altitude) that are smaller than those typically tracked and cataloged by the U.S. Space Surveillance Network. The Goldstone Orbital Debris Radar is an extremely sensitive sensor capable of detecting a 3 mm metallic sphere at 1000 km [1], which makes it an incredibly useful tool in the characterization of the sub-centimeter-sized debris population.

The Goldstone Orbital Debris Radar is located in the Goldstone Deep Space Communications Complex in the Mojave Desert near Barstow, California and is operated by NASA's Jet Propulsion Laboratory. It is a bistatic radar system, with one dish acting as a transmitter and another acting as a receiver. Historically, the Goldstone Orbital Debris Radar has used the 70-m DSS-14 "Mars" dish as the transmitter and the 34-m DSS-15 "Uranus" dish as the receiver. Originally operated in a near zenith-pointing configuration, the system has undergone a number of upgrades including a receiver bandwidth upgrade, a redesigned pointing geometry, and an addition of a second, independently triggered, orthogonal circular polarization receiver.

On 28 February 2018, DSS-15 was decommissioned. The 34-m "Apollo" antennas DSS-25 and DSS-26 were identified as potential receiving antenna replacements for DSS-15.

The baseline between DSS-14 and DSS-15 is approximately 497 m, which allowed that configuration to sample the entirety of LEO with a single pointing. The baseline between DSS-14 and DSS-25/DSS-26, as shown in Fig. 1, is approximately 9.4 km, which restricts the altitude range over which the transmitter and receiver beams intersect. Before DSS-15 was decommissioned, the pointing configuration consisted of DSS-14 pointing eastward at an elevation of 75 degrees with DSS-15 pointed such that the beam centers intersected at 550 km from DSS-14.

Currently, data is being taken with DSS-14 pointing eastward at an elevation of 75 degrees and either DSS-25 or DSS-26 pointed such that the beam centers intersect at 800 km from DSS-14, which roughly corresponds to the altitude regime with the highest debris flux. The normalized gain product, as a function of range from DSS-14, is shown in Fig. 2. Whereas DSS-14 and DSS-15 can cover LEO in a single pointing, DSS-14 and DSS-25 can only cover a roughly 100-km altitude extent.

In preparation for the decommissioning of DSS-15, a test was performed on 27 October 2017 in which both DSS-15 and DSS-25 were operated as receivers simultaneously. The experiment ran for 2.44 hours. During that time, DSS-15, operating at a system temperature of 14.35 °K, detected 87 objects in its principle polarization channel; DSS-25, operating at a system temperature of 39.98 °K, detected 41 objects in its principle polarization channel.

Current results indicate debris particles detected with DSS-25/DSS-26 will be ~45% of detected particles with DSS-15, due to smaller overlap in antenna beams.

Work to characterize efficacy of the newly configured Goldstone Orbital Debris Radar is ongoing. Although the particle detection rates are reduced due to the restricted intersection altitude range, the Goldstone Orbital Debris Radar still can prove invaluable in the characterization of the sub-centimeter debris population in LEO.

References

1. Folkner, W. M. "DSN station locations and uncertainties," *TDA Progress Report*, pp. 42-128, (1996).
2. Goldstein, S. J. and Goldstein, R. M. "Some properties of millimetric space debris," *The Astronomical Journal* 107, pp. 367-371, (1994).
3. Goldstein, R. M. "On the Flux of Millimetric Space Debris," *The Astronomical Journal*, 95-0382, JPL TRS 1992, URI: <http://hdl.handle.net/2014/29144>, (1995).
4. Goldstein, R. M., Goldstein, S. J., and Kessler, D. J. "Radar observations of space debris," *Planetary and Space Science* 46.8, pp. 1007-1013, (1998).
5. Matney, M., et al. "Recent results from Goldstone orbital debris radar," *Advances in Space Research* 23.1, pp. 5-12, (1999).
6. Slade, M., et al. "FY2018 MMOD Management Report," *Jet Propulsion Laboratory*, (2018). ♦

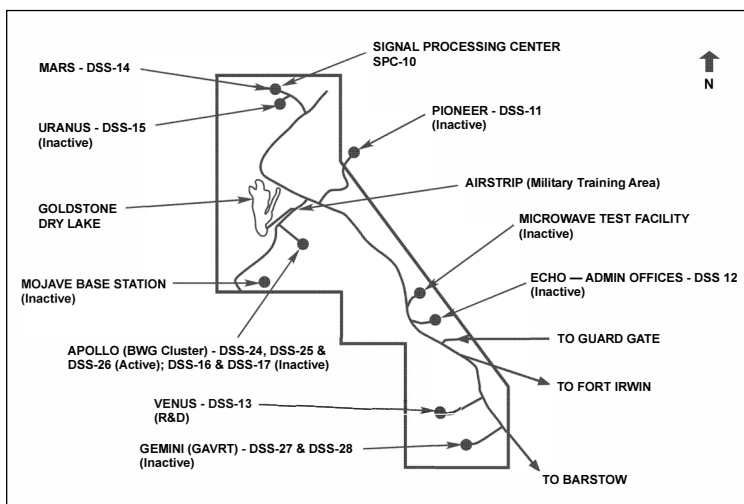


Figure 1. Map of Goldstone Deep Space Communications Complex with positions and operational standing of each antenna. Credit: Courtesy NASA/JPL-Caltech

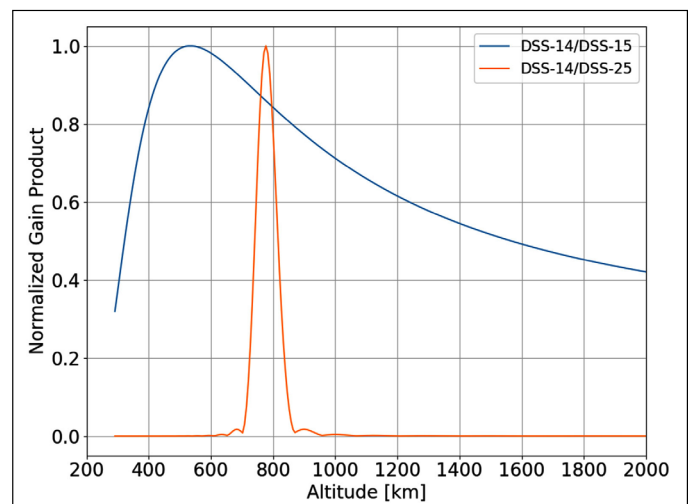


Figure 2. Normalized gain product versus altitude for the DSS-14/DSS-15 and DSS-14/DSS-25 observation configurations.

WORKSHOP REPORTS

2018 NASA-DOD Workshop, 16 October 2018, Houston, Texas, USA

The NASA-DOD Orbital Debris Working Group (ODWG) meeting was conducted 16 October 2018 by audioconference. This annual 1-day meeting reviews activities and research in orbital debris of mutual interest to both NASA and the Department of Defense (DOD). The OWDG originated in recommendations by interagency panels, who reviewed U.S. Government orbital debris activities in the late 1980s and early 1990s. This is the 21st working group meeting and was co-chaired by Dr. J.-C. Liou of NASA's Orbital Debris Program Office (ODPO) and Mr. Tim Payne from the Operational Assessments Division, HQ Air Force Space Command (AFSPC) A3/6Z.

During the meeting, NASA delivered seven presentations and the DOD delivered four presentations and led two additional discussions (no slides submitted). Dr. Liou discussed the history of the United Nations/Committee on the Peaceful Uses of Outer Space, Long-term Sustainability of Outer Space Activities; a summary from the recent Inter Agency Space Debris Coordination Committee (IADC); and reviewed on-going efforts to address the U.S. Space Policy Directive-3, the first National Space Traffic Management Policy; and update the U.S. Orbital Debris Mitigation Standard and Practices.

Dr. Sue Lederer presented the status of the Eugene Stansbery Meter-Class Autonomous Telescope (ES-MCAT) located at the John Africano NASA-AFRL Orbital Debris Observatory (on Ascension Island. This included ES-MCAT goals, FY18 accomplishments, and the project's current status, including the mirror recoating status and Initial Operation Capability completion. The presentation also showcased the install of the new dome and ringwall for the smaller 0.4-m telescope, designated the James R. Benbrook Telescope, co-located with ES-MCAT (refer to ODQN, vol 21, issue 1, February 2017, pp. 3-4).

Next, Dr. Tim Kennedy provided an overview and update regarding the new radar data processing software, Debris Radar Automated Data Inspection System (DRADIS), and the radars HUSIR/HAX and Goldstone. Initial operational capability for DRADIS was achieved in January 2018 and initial testing for full operational capability is expected by Q2 of FY19.

Dr. Liou presented an overview of the

Space Debris Sensor (SDS) and the current status update for the project. Also discussed was the path forward for future mission opportunities utilizing Debris Resistive/Acoustic Grid Orbital NASA-NAVY Sensor (DRAGONS) technology and lessons learned from SDS to address the millimeter-sized particles, particularly above 600 km altitude.

Dr. Mark Matney presented an overview of engineering models, specifically the NASA ODPO Orbital Debris Engineering Model (ORDEM) for space users. He reviewed the status on the development of ORDEM v. 3.1 and the plan forward for ORDEM 4.0 that will include new data, debris shape distributions, finer density distributions, and potential new model architecture.

Dr. Jack Bacon presented a background on U.S. Standards & Policies and updates to Procedural Requirement (NPR) 8715.6 Rev. B and ODPO's NASA Standard (NS) 8719.14B. Also discussed was the status of ODPO's Debris Assessment Software (DAS) 3.0 currently in beta testing, laboratory tests to improve ablation models that involve fiber-reinforced resins, and NASA's Object Reentry Survival Analysis Tool (ORSAT) improvements including optimization and modeling orbit reentry.

Finally, Dr. Heather Cowardin presented status and plans for continued analysis of the DebrisSat fragments and incorporating this data into ODPO computer models of the collisional breakup of a modern satellite in preparation for ORDEM 4.0. DebrisSat was a high-fidelity mock-up satellite constructed with modern satellite materials that was subject to a catastrophic hypervelocity impact in 2014. Fragments from the test are still being extracted from the soft-catch material that lined the vacuum chamber during the test. At the time of the presentation, more than 183,000 fragments had been recovered with over 30,000 characterized by the University of Florida, a DebrisSat consortium partner. Preliminary data was presented that showed the current cumulative number as a function of size, material, shape categories, and mass in relationship to the current NASA Standard Satellite Breakup Model.

Following the morning NASA presentations, Mr. Gary Wilson presented for Maj. Christian Abodeely, HQ AFSPC/A5S, on the current status of the Space Fence in Kwajalein, requirements for

the Space Fence, and overview of the current and expected performance for LEO-GEO. A brief overview of the Space Fence Evaluation of Radar Effectiveness (SFERES) project was presented, specifically the current schedule and primary stakeholders that will utilize small radar cross section (RCS) calibrated stainless steel spheres for ground-based calibration.

Mr. Doug Moffitt, HQ AFSPC/A3/6wS, presented an update on the Space Surveillance Network. An update on current and expected ground-based and in situ sensors that contribute to the SSN was discussed. Of high interest was the Geosynchronous Space Situational Awareness Program, the Operationally Responsive Space program, and the upcoming Space Surveillance Telescope that is being relocated to Australia.

Mr. Tim Payne discussed improvements to the SGP4 Deep Space algorithm. The analysis has exposed SGP4's Deep Space perturbation fidelity as a significant contributor of deep space uncorrelated targets and associated tagging anomalies that impact the SSN sensors and overall space situational awareness. Improvements are underway, including resolving compatibility issues, increasing run-time, and integrating it into various systems.

Mr. Ron Berkley, A3/6Z, presented the final charts on the proposed satellite catalog renumbering plan. To address the limited time that five digit satellite numbers will be available for cataloging targets, a nine digit numbering system was proposed that included three-line element sets (3LE). The proposed memo to accept the new numbering system was not approved and an alternative solution is underway. The Alpha-5 TLE is a stopgap measure that would utilize alpha numeric characters after the five digit catalog is exceeded. This is still under development and approval for implementation needs to be authorized.

The last two DOD topics were open discussions, the first led by Maj. Tyler Eske regarding ES-MCAT communication plans for allowing ES-MCAT data to be submitted as SSN data contributor and the last by Diana McKissock, 18 SPCS, discussing updates on space-track data sharing. ♦

NASA Aerospace Battery Workshop, 27-29 November 2018, Huntsville, AL, USA

The NASA Aerospace Battery Workshop was held from 27 to 29 November 2018 in Huntsville, Alabama, with about 100 participants from the global battery engineering community. This annual workshop is hosted by Marshall Space Flight Center, and sponsored by the NASA Engineering and Safety Center. The workshop consisted of five sessions, covering topics such as on-orbit battery performance, design-for-safety, fast charging, and thermal runaway testing.

This meeting report includes highlights of the conference, with emphasis on presentations relevant to ODQN readers. The first day featured presentations on reduced-order modeling of Nickel-Manganese-Cobalt Oxide (NMC) lithium-ion batteries, as well as an update on the replacement of older nickel-hydrogen batteries on the International Space Station with high-performance lithium ion batteries. The day ended with a presentation from Mr. Brad

Reed of the American Institute of Aeronautics and Astronautics (AIAA), “Status of Cell-Level AIAA S-144-201X Qualification, the New AIAA Battery-Level Qualification Standard, and Upcoming Changes to US Government Regulatory Requirements for Space Cells/Batteries,” discussing end-to-end standards for aerospace battery safety qualification. Day Two continued with presentations on fast charging, test and analysis methods, and design-for-safety. New designs for safer batteries and their initial test results were presented by KULR Technology (using wicking material to evaporate water to mitigate thermal runaway) and by ABSL Space Products (reduced mass yet higher thermal conductivity webbing for 18650 cell-based batteries).

The workshop closed with presentations on new cell and battery qualification from ABSL Space Products, Saft, and Mitsubishi Electric

Corporation, and battery performance history from Lockheed Martin Space, and Iridium Satellite LLC (Iridium). The presentation from Iridium was of historical significance, as the last operational spacecraft of the original Iridium constellation (launched 1997-2002) is due to be retired soon, and that constellation has not experienced any satellite losses attributable to their nickel-hydrogen batteries.

The NASA Aerospace Battery Workshop was a valuable opportunity for representatives from industry, academia, and government to assemble and discuss modeling capabilities, state-of-practice battery design and performance, as well as the latest research interests. Presentations from this and past workshops will be made available at <https://www.nasa.gov/batteryworkshop>. ♦

The 2018 Spacecraft Anomalies and Failures Workshop, 11-12 December 2018, Chantilly, Virginia, USA

The 2018 version of the National Reconnaissance Office/NASA (co-sponsored) SCAF Workshop focused on refining a process to further the tradecraft of anomaly/failure attribution to a root cause; a refinement facilitated by allocating more time for small group deliberations. From both the response of the attendees and the tangible feedback to the Lean Anomaly Attribution Framework, the gathering was a success. Twenty presentations over the 2-day workshop were provided to over 100 attendees each day. Attendees and presenters included representatives from academia, industry, civil, and military space organizations.

There were two overarching observations that will drive changes to the evolving common

anomaly attribution framework and guide planning for next year’s workshop.

First, the processing of anomalies and the importance of determining root cause is necessarily different for satellite operators, mission assurance practitioners, and satellite designers. However, there should be an established process by which these three communities share data amongst themselves for a specific program and (hopefully eventually) between civil, military, and commercial space communities. Specific discussions on both Day One and Day Two involved the benefit and necessity of having the operations people more aware of what forensics work is hoped to be done (*e.g.*, determine root cause anomaly/failure). It is equally critical for

mission assurance practitioners and data scientists to gain a better appreciation for the importance of timely anomaly resolution.

Second, the fact that most anomalies have multiple causes any anomaly attribution process that assumes a single trigger (or cause) for an anomaly or failure may be limiting. The general consensus was that while you might have a minor disruption from a single trigger (*e.g.*, solar flare or part failure) the eventual mission-reducing or mission-terminating event usually involves multiple triggers (*i.e.*, there may be more than one root cause). This is even more likely as a satellite ages. ♦

ABSTRACT FROM THE NASA ODPO

2019 Hypervelocity Impact Symposium (HVIS 2019), 14-19 April 2019, Destin, Florida, USA

Using the Debrisat fragments to update the NASA Standard Satellite Breakup Model and shape effects on ballistic limit equations

H. COWARDIN, P. ANZ-MEADOR, J. MURRAY, J.-C. LIOU, E. CHRISTIANSEN, M. SORGE, N. FITZ-COY, AND T. HUYNH

Existing DOD and NASA satellite breakup models are based on a key laboratory test, the

1992 Satellite Orbital debris Characterization Impact Test (SOCIT), which has supported many applications and matched on-orbit events involving older satellite designs reasonably well over the years. To update and improve these

models, the NASA Orbital Debris Program Office, in collaboration with the Air Force Space and Missile Systems Center, The Aerospace

continued on page 11

HVIS 2019

continued from page 10

Corporation, and the University of Florida, conducted a hypervelocity impact test using a high-fidelity mock-up satellite, DebrisSat, in controlled and instrumented laboratory conditions. DebrisSat is representative of present-day LEO satellites, having been constructed with modern spacecraft materials and techniques. The DebrisSat fragment ensemble provided a variety of shapes, bulk densities, and dimensions. Fragments down to 2 mm in size are being characterized by their physical and derived properties. A subset of fragments will be analyzed further in laboratory radar and optical facilities to update the existing radar-based NASA Size Estimation Model (SEM)

and develop a comparable optical-based SEM. Thoroughly understanding size estimates from ground-based optical and radar sensors is one of the key parameters used in assessing the environment and the risks that debris present to operational spacecraft. The data will inform updates to the current NASA Standard Satellite Breakup Model (SSBM), which was formulated using laboratory and ground-based measurements of on-orbit fragmentation events to describe an average breakup for spacecraft and upper stage collisions and explosions. DebrisSat will extend the laboratory data ensemble. The DebrisSat shape and density categories provide a baseline for non-

spherical projectile hypervelocity impact testing for damage assessment. The data from these tests, simulations, and analyses will be used to update the NASA Orbital Debris Engineering Model (ORDEM) with more realistic simulations of catastrophic fragmentation events for modern satellites and to assess the risk posed by the orbital debris environment. This paper provides an overview of the project, updates on the characterization process, and the NASA analysis status. ♦

UPCOMING MEETINGS

15-17 May 2019: 10th International Association for the Advancement of Space Safety (IAASS) Conference, El Segundo – Los Angeles, California, USA

The 10th conference of the IAASS has as its theme “Making Safety Happen.” Major debris-related topics include designing safety into space vehicles, space debris remediation, re-entry safety, nuclear safety for space missions, safety risk management

and probabilistic risk assessment, and launch and in-orbit collision risk. In addition to the main sessions, four specialized sections will address Space Debris Reentries, Space Traffic Management, Safety Standards for Commercial Human Spaceflight, and Human Performance

and Safety. Abstract submission deadline for the conference passed on 7 December 2018. Additional information for the 2019 IAASS is available at <http://iaassconference2019.space-safety.org/>.

15-21 June 2019: 32nd International Symposium on Space Technology and Science, Fukui, Japan

The 32nd ISTS will be held in June 2019 in conjunction with the 9th Nano-Satellite Symposium (NSAT). This year’s conference will be convened under the theme of “Fly like a Phoenix to Space.” Technical sessions include,

but are not limited to, Space Environment and Debris; Space Situational Awareness; Reentry Safety; Hypervelocity Impact; Debris Risk Assessment and Management; Debris Mitigation and Removal; Space Law, Policy and

International Cooperation; and Space Traffic Management. The abstract submission deadline passed on 31 October 2018. Additional information about the conference is available at <http://www.ists.or.jp/index.html>.

3-8 August 2019: 33rd Annual Small Satellite Conference, Logan, Utah, USA

Utah State University (USU) and the AIAA will sponsor the 33rd Annual AIAA/USU Conference on Small Satellites at the university’s Logan campus, Utah, USA. With the theme of “Driving a Revolution,” the 33rd conference will explore technical

and development issues and the unique opportunities that arise from missions composed of tens, hundreds, or thousands of small satellites. Session topics include a review of the past 18 months of SmallSat activity, a preview of the next 18 months, ground

systems, space access, educational programs, advanced technologies, and science/mission payloads. The abstract submission deadline passed on 1 February 2019. Additional information about the conference is available at <https://smallsat.org/>.

17-20 September 2019: 20th Advanced Maui Optical and Space Surveillance Technologies Conference, Maui, Hawaii, USA

The technical program of the 20th Advanced Maui Optical and Space Surveillance Technologies Conference (AMOS) is anticipated to focus on subjects that are mission critical to Space Situational

Awareness. The technical sessions include papers and posters on Orbital Debris, Space Situational Awareness, Adaptive Optics & Imaging, Astrodynamics, Non-resolved Object Characterization, and related topics. Abstract

submission deadline passed on 1 March 2019. Additional information about the conference is available at <https://amostech.com> and this announcement will be updated in the ODQN as details become available.

UPCOMING MEETINGS - Continued

21-25 October 2019: 70th International Astronautical Congress (IAC), Washington, D.C., USA

The IAC will convene in Washington, D.C., in 2019 with a theme of “Space: the Power of the Past, the Promise of the Future.” The IAA will organize the 17th Symposium on Space Debris as session A6 during the congress. Nine dedicated sessions are

planned to cover all aspects of orbital debris activities, including measurements, modeling, hypervelocity impact, mitigation, remediation, and policy/legal/economic challenges for environment management. An additional joint session with the section B4.10 Small Satellites

will be conducted to promote the long-term sustainability of space. Session A6 will also include an interactive presentation. The abstract submission deadline passed on 13 March 2019. Additional information for the 2019 IAC is available at <https://www.iac2019.org/>.

9-12 December 2019: The First International Orbital Debris Conference (IOC), Sugar Land, Texas, USA

The first of this “once-every-4-years” conference series will be initiated 9-12 December 2019 in Sugar Land (greater Houston area), Texas, United States. The goal of the conference is to highlight orbital debris research activities in the United States and to foster collaborations with the international

community. The 4-day conference will cover all aspects of micrometeoroid and orbital debris research, mission support, and other activities. Topics to be covered include radar, optical, in situ, and laboratory measurements; engineering, long-term environment, and reentry modeling; hypervelocity impacts

and protection; and mitigation, remediation, policy, and environment management. The abstract submittal deadline passed on 22 April 2019. The conference announcement is available at <https://www.hou.usra.edu/meetings/orbitaldebris2019/>.

14-16 January 2020: 2nd International Academy of Astronautics (IAA) Conference on Space Situational Awareness (ICSSA), Washington, D.C., USA

The International Academy of Astronautics (IAA), the American Institute of Aeronautics and Astronautics (AIAA), and the University of Florida’s Mechanical and Aerospace Engineering Dept. will convene the 2nd IAA Conference on Space Situational

Awareness in Washington, D.C., USA. Technical sessions include, but are not limited to, resident space object and Near Earth Object sensing, identification, forecasting, tracking, proximity operations, risk assessment, debris removal, drag assisted reentry, and deorbiting

technologies. The abstract submission deadline is 15 August 2019. Additional information about the conference is available at <http://reg.conferences.dce.ufl.edu/ICSSA/>.

INTERNATIONAL SPACE MISSIONS

01 October – 31 March 2019

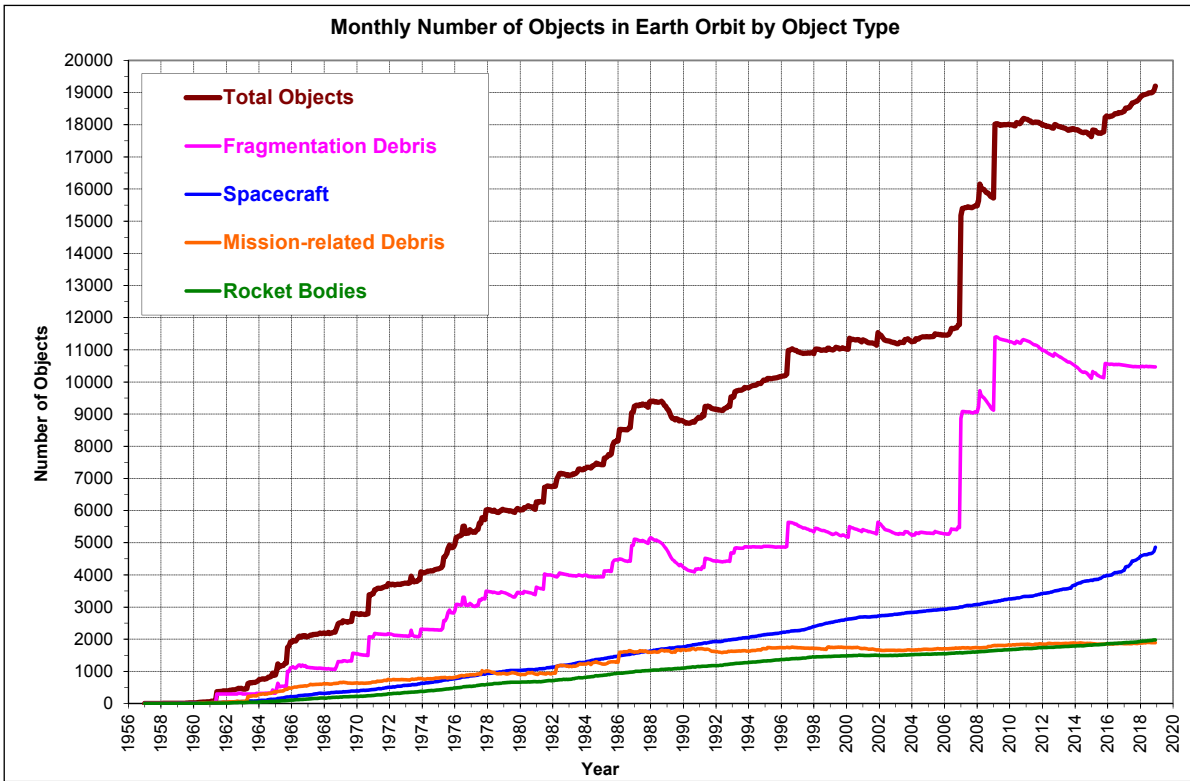
Intl.* Designator	Payloads	Country/Organization	Perigee Alt. (KM)	Apogee Alt. (KM)	Incl. (DEG)	Addnl. PL	Earth Orbital R/B	Other Cat. Debris
1998-067	ISS dispensed payloads	various	395	400	51.64	4	0	0
2018-076A	SAOCOM 1-A	ARGENTINA	621	624	97.89	0	0	0
2018-077A	YAOGAN-32 A	CHINA	695	697	98.25	0	0	1
2018-077B	YAOGAN-32 B	CHINA	695	697	98.25			
2018-078A	BEIDOU 3M15	CHINA	21504	21551	55.08	0	2	0
2018-078B	BEIDOU 3M16	CHINA	21511	21545	55.08			
2018-079A	AEHF 4 (USA 288)	USA	35769	35803	4.75	0	1	0
2018-080A	BEPICOLOMBO	ESA	EN ROUTE TO MERCURY			0	0	0
2018-081A	HAIYANG 2B	CHINA	965	968	99.35	0	1	3
2018-082A	COSMOS 2528	RUSSIA	901	910	67.15	0	1	0
2018-083A	CFOSAT	CHINA	516	518	97.52	6	1	0
2018-084B	GOSAT 2	JAPAN	615	617	97.83	5	1	7
2018-085A	BEIDOU 3G1	CHINA	35781	35790	2.75	0	1	0
2018-086A	COSMOS 2529 (GLONASS)	RUSSIA	19109	19151	64.75	0	1	0
2018-087A	METOP-C	ELUME	819	822	98.71	0	0	0
2018-088A	CICERO 10	USA	496	519	85.04	6	1	0
2018-089A	GSAT 29	INDIA	35777	35795	0.02	0	1	0
2018-090A	ESHAIL 2	QATAR	35779	35794	0.02	0	1	0
2018-091A	PROGRESS MS-10	RUSSIA	408	411	51.64	0	1	0

* Intl. = International; PL = Payloads; Alt. = Altitude; KM = kilometers; Incl. = Inclination; DEG = degrees; Addnl. = Additional; R/B = Rocket Bodies; Cat. = Cataloged

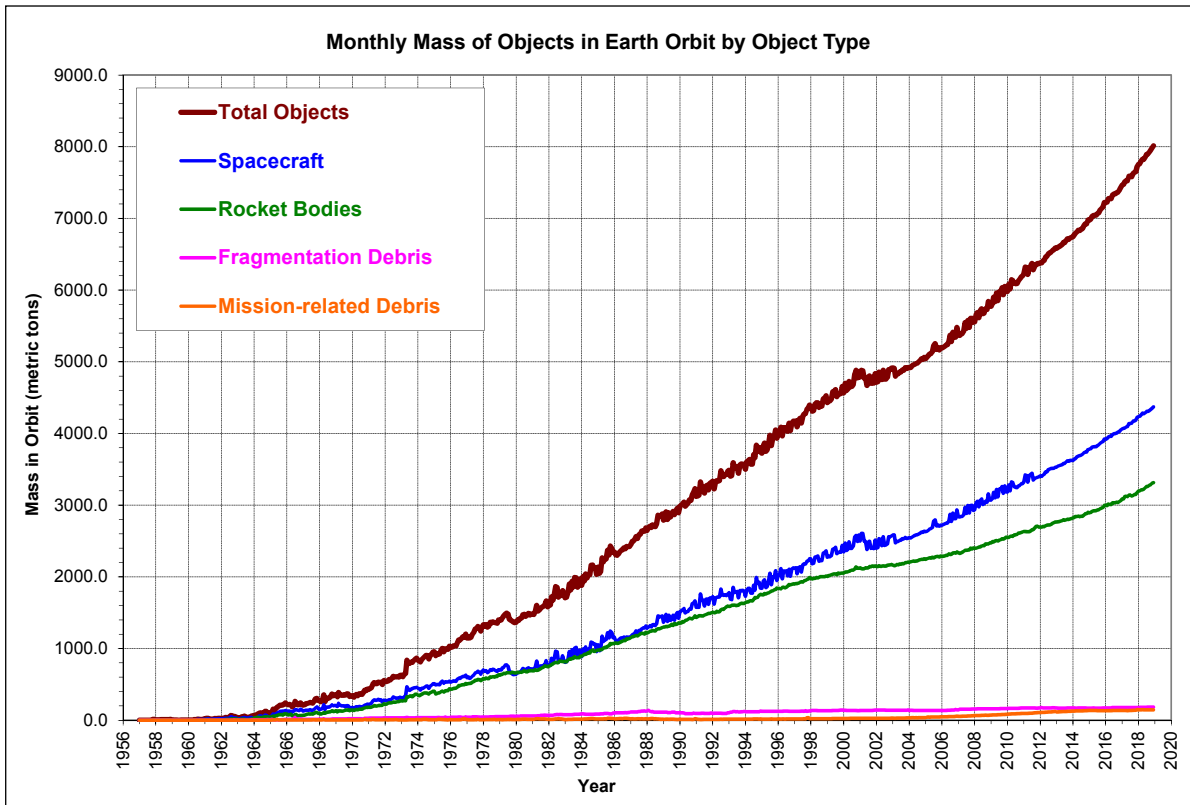
missions continued on page 14

DAS 2.1 NOTICE

Attention DAS 2.1 Users: an updated solar flux table is available for use with DAS 2.1. Please go to the Orbital Debris Website at <https://www.orbitaldebris.jsc.nasa.gov/mitigation/debris-assessment-software.html> to download the updated table and subscribe for email alerts of future updates.



Monthly Number of Cataloged Objects in Earth Orbit by Object Type. This chart displays a summary of all objects in Earth orbit officially cataloged by the U.S. Space Surveillance Network. "Fragmentation debris" includes satellite breakup debris and anomalous event debris, while "mission-related debris" includes all objects dispensed, separated, or released as part of the planned mission.



Monthly Mass of Objects in Earth Orbit by Object Type. This chart displays the mass of all objects in Earth orbit officially cataloged by the U.S. Space Surveillance Network.

SATELLITE BOX SCORE

(as of 01 April 2019, cataloged by the
U.S. SPACE SURVEILLANCE NETWORK)

Country/ Organization	Payloads*	Rocket Bodies & Debris	Total
CHINA	346	3673	4019
CIS	1524	5063	6487
ESA	89	56	145
FRANCE	64	492	556
INDIA	95	118	213
JAPAN	175	115	290
USA	1750	4792	6542
OTHER	929	123	1052
TOTAL	4972	14432	19404

* active and defunct

INTERNATIONAL SPACE MISSIONS - Cont.

01 October – 31 March 2019

Intl.* Designator	Payloads	Country/ Organization	Perigee Alt. (KM)	Apogee Alt. (KM)	Incli. (DEG)	Addnl. PL	Earth Orbital R/B	Other Cat. Debris
2018-092A	CYGNUS NG-10	USA	300	316	51.64	5	1	0
2018-093A	BEIDOU 3M17	CHINA	21507	21549	54.9	0	2	0
2018-093B	BEIDOU 3M18	CHINA	21510	21546	54.91			
2018-094A	OBJECT A	CHINA	485	506	97.41	4	0	3
2018-095A	MOHAMMED VI-B	MOROCCO	637	640	97.94	0	0	0
2018-096A	HYSIS	INDIA	628	640	97.96	30	1	0
2018-097A	COSMOS 2530	RUSSIA	1479	1510	82.51	1	1	0
2018-097B	COSMOS 2531	RUSSIA	1480	1509	82.52			
2018-097C	COSMOS 2532	RUSSIA	1479	1510	82.51			
2018-098A	SOYUZ MS-11	RUSSIA	408	411	51.64	0	1	0
2018-099A	MINXSS-2	USA	571	592	97.75	63	0	1
2018-100A	GEO-KOMPSAT-2A	SOUTH KOREA	35779	35795	0.04	0	1	1
2018-100B	GSAT 11	INDIA	35761	35812	0.03			
2018-101A	DRAGON CRS-16	USA	395	405	51.64	0	0	3
2018-102A	SAUDISAT 5A	SAUDI ARABIA	534	552	97.61	10	1	1
2018-102C	SAUDISAT 5B	SAUDI ARABIA	532	551	97.61			
2018-103A	CHANG'E 4	CHINA			LUNAR LANDER	0	0	0
2018-104A	AEROCUBE 11-R3	USA	491	512	85.03	12	2	0
2018-105A	GSAT 7A	INDIA	35777	35797	0.05	0	1	0
2018-106A	CSO-1	FRANCE			NO ELEMS.AVAILABLE	0	0	0
2018-107A	COSMOS 2533	RUSSIA	35779	35793	0.01	0	1	1
2018-108A	HONGYUN 1	CHINA	1061	1079	99.92	0	1	0
2018-109A	NAVSTAR 77 (USA 289)	USA	20168	20199	55	0	0	0
2018-110A	TJS-3	CHINA	35780	35795	0.12	0	2	0
2018-111A	KANOPUS-V 5	RUSSIA	505	510	97.46	25	0	5
2018-111B	KANOPUS-V 6	RUSSIA	507	511	97.46			
2018-111Q	GRUS-1A	JAPAN	572	584	97.72			
2018-112A	YUNHAI 2 1	CHINA	516	525	50.01	0	1	0
2018-112B	YUNHAI 2 2	CHINA	796	803	50.01			
2018-112C	YUNHAI 2 3	CHINA	512	524	50.01			
2018-112D	YUNHAI 2 4	CHINA	1088	1098	50.01			
2018-112E	YUNHAI 2 5	CHINA	796	804	50.01			
2018-112F	HONGYAN 1	CHINA	1090	1101	50.01			
2018-112G	YUNHAI 2 6	CHINA	1092	1100	50.01			
2019-001A	CHINASAT 2D	CHINA	35782	35791	0.05	0	1	0
2019-002A	IRIDIUM 180	USA	775	780	86.4	0	0	0
2019-002B	IRIDIUM 176	USA	652	655	86.62			
2019-002C	IRIDIUM 168	USA	776	779	86.4			
2019-002D	IRIDIUM 173	USA	776	779	86.4			
2019-002E	IRIDIUM 169	USA	760	766	87.41			
2019-002F	IRIDIUM 172	USA	776	779	86.4			
2019-002G	IRIDIUM 175	USA	652	656	86.61			
2019-002H	IRIDIUM 171	USA	776	779	86.4			
2019-002J	IRIDIUM 170	USA	655	655	86.62			
2019-002K	IRIDIUM 167	USA	775	780	86.4			
2019-003A	RAPIS-1	JAPAN	498	513	97.29	6	1	0
2019-004A	USA 290	USA			NO ELEMS.AVAILABLE	0	0	0
2019-005B	JILIN-01-09	CHINA	520	542	97.51	2	1	0
2019-005E	JILIN-01-10	CHINA	516	545	97.51			
2019-006A	MICROSAT-R	IND	260	282	96.64	1	1	0
2019-007A	SAUDIGEOSAT1/HELLASAT4	GREC			EN ROUTETO GEO	0	1	1
2019-007B	GSAT-31	IND	35774	35799	0.04			
2019-008A	EGYPTSAT A	EGYP	653	655	98.01	0	0	0
2019-009A	NUSANTARA SATU	INDO	35777	35797	0.03	2	1	1
2019-010A	ONEWEB-0012	UK	988	1016	87.77	0	0	0
2019-010B	ONEWEB-0010	UK	988	1014	87.77			
2019-010C	ONEWEB-0008	UK	988	1014	87.77			
2019-010D	ONEWEB-0007	UK	988	1013	87.77			
2019-010E	ONEWEB-0006	UK	988	1012	87.77			
2019-010F	ONEWEB-0011	UK	988	1009	87.77			
2019-011A	CREW DRAGON DEMO-1	USA	393	400	51.64	0	0	1
2019-012A	CHINASAT 6C	CHINA	35774	35798	0.09	0	1	0
2019-013A	SOYUZ MS-12	RUSSIA	408	411	51.64	0	1	0
2019-014A	WGS 10 (USA 291)	USA	26479	45100	0.21	0	0	0
2019-015A	PRISMA	ITALY	617	620	97.9	0	0	0
2019-016A	R3D2	USA	422	438	39.52	0	2	0
2019-017A	TIANLIAN 2-01	CHINA			EN ROUTETO GEO	0	1	0

* Intl. = International; PL = Payloads; Alt. = Altitude; Incl. = Inclination; Addnl. = Additional; R/B = Rocket Bodies; Cat. = Cataloged

Visit the NASA
Orbital Debris Program Office
Website

www.orbitaldebris.jsc.nasa.gov

Technical Editor
Phillip Anz-Meador, Ph.D.

Managing Editor
Debi Shoots



Correspondence concerning
the ODQN can be sent to:

NASA Johnson Space Center
The Orbital Debris Program Office
X15-B9E/Jacobs
Attn: Debi Shoots
Houston, TX 77058



debra.d.shoots@nasa.gov



National Aeronautics and Space Administration
Lyndon B. Johnson Space Center
2101 NASA Parkway
Houston, TX 77058

www.nasa.gov
<https://orbitaldebris.jsc.nasa.gov/>